12

INJURY BIOMECHANICS RESEARCH
Proceedings of the Thirty-First International Workshop

Comparison of Cadaveric Human Head Mass Properties: Mechanical Measurement vs. Calculation from Medical Imaging

C. Albery and J. J. Whitestone

ABSTRACT

In order to accurately simulate the dynamics of the head and neck in impact and acceleration environments, valid mass properties data for the human head must exist. The mechanical techniques used to measure the mass properties of segmented cadaveric and manikin heads cannot be used on live human subjects. Recent advancements in medical imaging allow for three-dimensional representation of all tissue components of the living and cadaveric human head that can be used to calculate mass properties. A comparison was conducted between the measured mass properties and those calculated from medical images for 15 human cadaveric heads in order to validate this new method. Specimens for this study included seven female and eight male, unembalmed human cadaveric heads (ages 16 to 97; mean = 59±22). Specimen weight, center of gravity (CG), and principal moments of inertia (MOI) were mechanically measured (Baughn et al., 1995, Self et al., 1992). These mass properties were also calculated from computerized tomography (CT) data. The CT scan data were segmented into three tissue types - brain, bone, and skin. Specific gravity was assigned to each tissue type based on values from the literature (Clauser et al., 1969). Through analysis of the binary volumetric data, the weight, CG, and MOIs were determined. The medical image data compared with the mechanically measured data resulted in the following errors: 0.4% to 6% (mean = 2.8%) for weight, 0.01 cm to 0.34 cm (mean = 0.1 cm) for the CG, 0.1% to 10.4% (mean = 5.2%) for the MOIs. Medical image calculations for weight had significant ($p = 0.0074$) positive bias, as they did for two of the three MOIs (Ixx: $p = 0.0074$, Iyy: $p = 0.0010$). Medical imaging analysis proved to be a valid and accurate noninvasive method to calculate human head mass properties.

INTRODUCTION

The human body's response to excessive accelerations and impact is largely dependent on the body's inertial properties and any encumbering equipment. Without doubt, the head and neck are among the most exposed elements of the body in these harsh dynamic environments. This issue has been recognized by the government and within the medical and commercial communities for several decades. A great deal of research has been performed on characterizing the inertial properties of the heads and necks of cadavers and living humans (Harless, 1860; Clauser et al., 1969; Becker 1972; Walker et al., 1973; Chandler et al., 1974; Beier et al., 1980; McConville et al., 1980; Kaleps et al., 1984).

Within the United States Air Force, devices that encumber the head and neck often include helmets, oxygen masks, and helmet-mounted optics, especially for an aircrew member. The mass properties and the mass distribution of these devices relative to the head are critical design parameters for helmets and head-supported equipment. These parameters could affect the comfort, fit, performance and crash or ejection safety of head-mounted equipment. The distribution of head-supported mass may also affect the fatigue experienced by aircrew members. The mass properties parameters which have been identified as most important when designing helmet systems are total head-supported weight, moments of inertia (MOI), and the center of gravity (CG) location of the head-supported equipment (Knox et al., 1992, Self et al., 1992, Whitestone et al., 1996). Likewise, for advanced computations and accurate dynamic modeling, it is essential to have a prior knowledge of the mass properties of these equipment simulated in the model (Schultz et al., 1997, Beier et al., 1980).

BACKGROUND

This research was made possible due to a Cooperative Research and Development Agreement (CRADA) between the US Air Force Research Laboratory's Biodynamics and Acceleration Branch (AFRL/HEPA) and the University of Washington's Orthopaedic & Biomechanics Lab (UW-OBL). One of the primary missions of AFRL/HEPA is to conduct experimental research to define the human response to transient biodynamic stresses such as impact acceleration and aerodynamic forces. With the goal of developing aeromedical injury tolerance criteria, it is essential to understand the envelope of dynamic stresses within which the human body can operate without injury. Towards establishing these criteria, the experimental research often includes the exposure of human volunteers to a defined range of acceleration pulses. In order to accurately develop these criteria and successfully model the head and neck reaction to these pulses, it is important to have an accurate record of the mass properties of volunteer-subjects' heads. Since it is impossible to directly measure the subjects' head mass properties accurately without segmentation, it would be very helpful to develop a method for computing the head mass properties of the living human. Hence, the current studies were conducted to investigate the potential for using computed tomography (CT) analysis to accurately calculate the inertial properties of the living human head. Another application of this methodology is custom-fit and ballasted helmets to lessen the risk of increased bending and rotational moments due to an offset of the current head CG.

Due to recent advancements in medical imaging, we can now provide three-dimensional representations of CT data. Live human heads can now be volume rendered. Segmentation of tissue types including brain matter, fat, bone, and skin will allow for a morphological map of the head to which mass densities can be assigned. These segmented volumes can then be used to determine mass properties of the whole head.

To determine the reliability of using electronic imaging to determine mass properties, a commercial mass properties measurement system with known accuracy (Self et al., 1992) was used to directly measure and validate the imaging results. Our immediate objectives were to develop a methodology to directly measure the weight and CG of cadaveric human head specimens, and to develop the methodology for calculating the mass properties of these specimens using CT analyses. Once these methodologies are proven accurate and reliable, the ultimate goal of verifying the efficacy for using CT analysis to accurately calculate the mass properties of the living human head will be completed. This will lead to the development of a useful database of human head mass properties and anthropometry. The results of these two procedures will provide human head mass properties data, both measured and calculated, with respect to a head anatomical coordinate system.

METHODS

Specimens

Eight male and seven female cadaver specimens were measured. The male specimens ranged in age from 16-80 years at time of death, with a mean age of 55±22. The female specimens ranged in age from 23-97 years at time of death, with a mean age of 62±24. Overall (both male and female), the specimens ranged in age from 16-97 years at time of death, with a mean age of 59±22.

All specimens were acquired from the International Institute for the Advancement of Medicine (IIAM), Scranton, PA. Before delivery, all specimens were scanned for blood-borne pathogens, such as hepatitis and HIV. The specimens were ordered and received with at least the neck (cervical spine) still attached to the head. The necks were used in another concurrent study. Therefore, in order for the specimens to be considered, they had to have no history of head or neck trauma. The head and neck specimens were radiographed for gross degenerative changes or abnormalities and visually inspected for confounding pathologies. Any specimens not meeting our requirements were rejected. All specimens were handled according to Center for Disease Control (CDC) guidelines upon delivery. All specimens remained frozen (-20°C) until they were used in the study, at which time they were thawed according to the requirements for that particular part of the study. All specimens were naturally drained, and were not flushed nor embalmed.

Mass Properties: Direct Measurement

Procedural overview: The procedure consists of measuring the combined weight and CG of a specimen secured within a support box, and then measuring the properties of the support box by itself. The contribution from the support box is then subtracted from the combination, resulting in the weight and CG of the specimen alone. All predetermined landmarks on the head were then digitized in order to generate a head anatomical coordinate system and to acquire the data necessary to calculate various anthropometry. The CG location of each specimen was calculated with respect to a head anatomical axis system. The head anatomical axis system was used to locate the position of the CG with respect to the head and was defined by anatomical landmarks on the surface of the head and face. In addition, basic anthropometric measures were recorded, such as head circumference, head breadth, and head length.

Equipment: The direct measurement procedure included a three-sided orthogonal support box to secure the specimen during testing; a digital balance and moment table to determine the weight and CG; a three-dimensional digitizer to determine the anatomical coordinate system and location of the predetermined anatomical landmarks; anthropometric tools, such as ribbon tape, and calipers to perform basic anthropometry; and a computer for data acquisition and analysis.

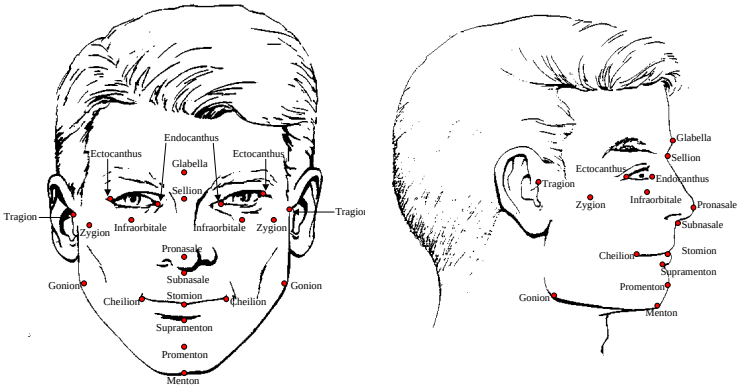

Figure 1: Anatomical features recorded

Marking the anatomical features: The first step was to thaw the specimen until the skin was palpable. The specimen was then shaved, cleaned and dried. Approximately 35 predetermined anatomical features were located by palpating the flesh and marked with permanent ink (Figure 1). Lead markers commonly used in radiographs were placed on key landmarks and were used to set up the specimen's head anatomical coordinate system. The landmarks identified, marked, and recorded were chosen either to satisfy the requirements for generating the anatomical coordinate system or to determine physical anthropometric dimensions for comparison to previous studies. Some of the landmarks not shown on Figure 1 include the apex, occiput, nuchale, and occipital condyles, as well as three reference landmarks on the forehead.

The head anatomical coordinate system: This system is based on the Frankfort plane of the head. Locating, marking with the lead markers, and digitizing four key landmarks generates this plane. The Y axis of the head anatomical coordinate system (positive to the left) is generated by digitizing the left and right tragions, located at the notch just above the tragus of the left and right ear. A vector from the right infraorbitale normal to the Y axis establishes the X axis of the head anatomical coordinate system (positive toward the front). The infraorbitale is located at the lowest point on the inferior margin of the orbit of the right eyesocket. The origin of the head anatomical coordinate system is at the intersection of these axes with the Z axis positive upward. The coordinate system is finally translated to the mid-sagittal plane of the head by digitizing the sellion (located at the greatest indentation of the nasal root depression) (Figure 2).

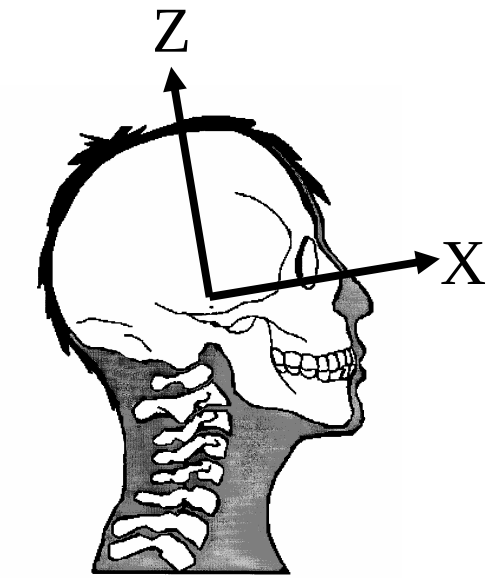

Figure 2**:** Head anatomical coordinate system

Dissection of the neck from the head: The head and neck went through a three-step dissection technique. This multi-phase technique was necessary due to the concurrent neck research. A portion of the head had to remain intact (attached to the neck) until the neck testing was complete. This segmentation included a posterior-to-anterior cut from the occipital protuberance to the zygomatic process and sphenoid bone (Figure 3A). Then an inferior-to-superior cut completed the initial segmentation (Figure 3B). Upon completion of the neck testing, the portion of the skull was reattached using adhesive (Figure 3C). The final segmentation was performed utilizing a technique much like that of past cadaveric head mass properties studies (Walker et al., 1973, Beier et al., 1980). This cut originates just below the external occipital protuberance, proceeding anteriorly and inferiorly to the atlantooccipital joint, then onto prevertebral muscle mass, intersecting with a cut just superior to the

hyoid bone that extends cranially and posteriorly (Figure 3D).

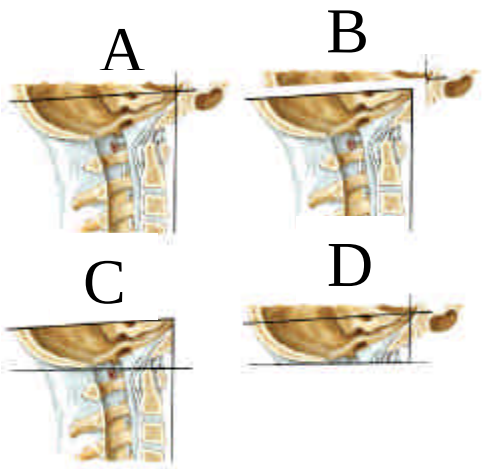

Figure 3: (A & B) Initial dissection of the head from the neck to allow a portion of the skull to remain attached to the neck for the concurrent neck study. (C) Reattachment of the portion of the skull. (D) Final segmentation separates the head and neck.

Securing the head within the support box: In order to directly measure the mass properties, the specimen was first mounted in a lightweight orthogonal support box. The three sides of the support box form mutually perpendicular planes that form the X, Y and Z axes, with the corner designated as the origin. Hook-and-loop straps or strips of tape were used to hold the specimen tightly within the box. The box properties are predetermined and later subtracted, leaving just the specimen properties. The box not only serves as a means for fixing the specimen during testing, it also serves as a source from which all the data are initially referenced.

Weight and CG determination: The weight of the specimen was determined by placing the specimen and support box on an electronic balance and recording the weight (Figure 4).

Figure 4: Manikin head within the support box being measured for CG_X

The CG location was determined with the use of the balance and a moment table assembly. The moment table is an aluminum plate supported by two steel knife-edge blades with their edges parallel to

each other and separated by a known distance. An aluminum chock is secured to the top of the plate directly above one of the steel blades. During testing, the chock side of the table is placed on an adjustable stand and the other side is placed on the electronic balance. The stand is adjusted until the table is level, and then the balance is zeroed. The force of the first moment of the specimen within the box along each axis is determined directly from the balance reading. With the weight of the specimen within the box as well as the blade-to-blade horizontal separation distance, the position of the composite center of gravity is calculated using summation of moments about the chock edge and results in

$$X_{CG} = \frac{F_S R_S}{F_{CG}} \tag{1}$$

where F_S = Balance reading of specimen within the support box on the moment table (converted to weight)

F_{CG} = Weight of the specimen within the support box

R_S = Known moment arm blade separation distance

X_{CG} = CG coordinate of specimen within the support box with respect to the support box in contact with the chock

To determine the CG of the specimen alone, the entire procedure was repeated for the empty support box. The empty support box CG was then subtracted from the combined specimen and box data, resulting in the CG of the specimen. Since first moments are additive, the center of gravity of the specimen with respect to the support box axis system is determined by subtracting the support box contribution:

$$X_T = \frac{F_{CG} X_{CG} - F_B X_B}{F_T} \tag{2}$$

where F_T = Weight of the specimen

F_{CG} = Weight of the specimen within the support box

F_B = Weight of the support box

X_T = X-axis CG location of the specimen

X_{CG} = X-axis CG location of the specimen within the support box

X_B = X-axis CG location of the support box.

This procedure is repeated for the Y- and Z-axis CG locations.

Coordinate system transformation: To this point, the measurements were located with respect to the box coordinate axes. To reference the properties of the specimen to a head anatomical coordinate system, the specimen landmarks were digitized with respect to the box coordinate system (box edges) using the electronic position coordinate digitizer. The box origin, located at the rear and right-hand corner of the outer box, and points representing the X, Y, and Z axes of the box (box edges) were digitized along with all the pre-marked head and face landmarks (Figure 5). Those points not accessible due to the frame of the box were digitized upon removal of the box along with at least three points from the previous set, allowing for inclusion in the final data set.

Mass Properties: Computed Tomography (CT) Protocol

Overview: Fifteen unembalmed cadaver heads were used for estimating mass properties. The spiral CT data were collected by the University of Washington's Orthopaedic & Biomechanics Lab,

Figure 5: Manikin head and helmet within support box being

located at the Harborview Medical Center, Seattle, WA. These data were transferred electronically to Total Contact Inc., Germantown, OH for segmentation and determination of mass properties using a combination of Analyze AVW developed by the Mayo Clinic, Microsoft Excel and Integrate, and Silicon Graphics visualization freeware developed by the Air Force.

CT imaging: The CT imager used was the GE High Speed Advantage System. This system has an X-ray strength of 120kV at 80mA. With both slice collimation (thickness) and table feed set at 1 mm, the following are the resultant dimensional resolutions:

- 1-D resolution = 273 mm circle at 512 pixels = 0.5332 mm/pixel
- 2-D resolution = 273 mm x 273 mm at 512 pixels x 512 pixels = 0.2843 $mm^2/pixel^2$
- 3-D resolution = 273 mm x 273 mm x 1 mm at 512 pixels x 512 pixels x 1 pixel = 0.2843 $mm^3/pixel^3$ = 0.2843 mm^3/voxel

Figure 6 shows an example slice of spiral CT data. The image is represented as a gray scale image and shows the 2-D view of the head. Likewise, the image shows the density phantom (product information), lead marker, as well as the bone, brain, and soft tissue. Contrary to this image, all scans were performed with the head in the prone position and progressed caudad.

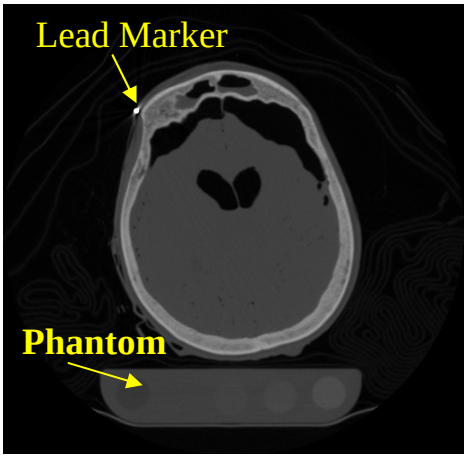

Figure 6: Slice of spiral CT data with lead marker and phantom

Image processing:

Segmentation of the image data was accomplished using Analyze AVW developed by the Mayo Clinic. This particular version was located at the Department of Radiology at the University of Iowa. Analyze is used to process medical images and was developed over the last 10 years by a team of physicians, biomedical engineers, and programmers at the Mayo Clinic. Analyze contains advanced automated segmentation routines including thresholding, 2-D and 3-D region growing, automated boundary detection, and morphological processing. Analyze provides a visualization interface for multi-tasking of medical images as shown in Figure 7.

Figure 7: Example of Analyze AVW visualization and analysis capability

The image data were transferred in DICOM format. As the volumetric data were fairly large, the DICOM slice data had to be entered into Analyze 50 slices at a time and later concatenated. The CT data were sampled to determine the range of Hounsfield units for bony structure. The skull was segmented by thresholding the bone using a range of –99 to 200. A binary map of the skull was created and saved for use with the conditional dilation.

The images were then eroded and connected until the brain was separated from the skull. The erosion was performed as a morphological operator on the two-dimensional images. The erosion element was a 3x3x3 rectilinear structuring element. The connect operation was performed on the volumetric data as shown in Figure 8.

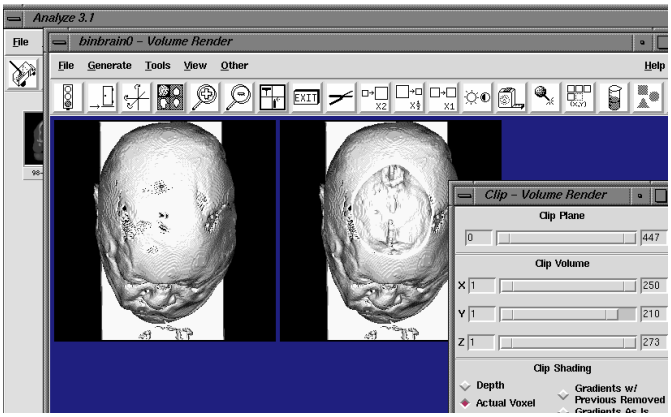

Figure 8: Clipping step: sometimes necessary in order to connect the voxels subscribing to “brain” volumetrically

After completely separating the brain from the skull, the binary brain was conditionally dilated (one more time than the number of erosion operations) using the original binary image to expand the brain to its original size as shown in Figures 9 and 10.

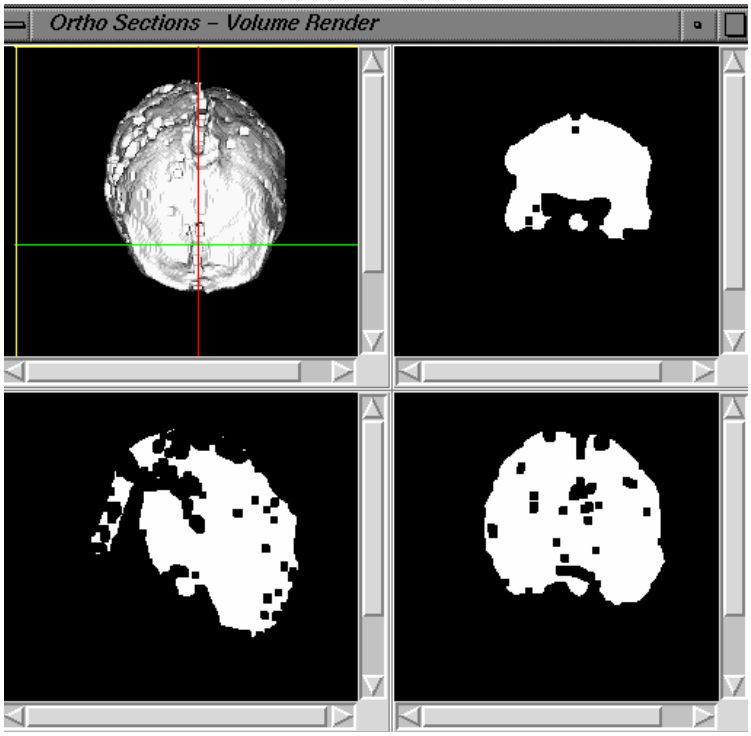

Figure 9: The eroded brain before dilation. The cross sections demonstrate the binary nature of this image.

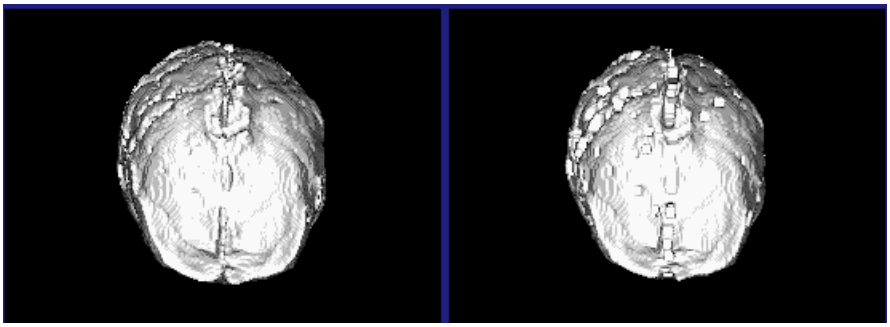

Figure 10: The brain after dilation and before dilation. The brain has a smooth surface due to the freezing process used with the cadaver heads.

The dilated binary brain was saved as the brain object in the object map corresponding to the subject. The anatomical landmarks were selected by thresholding the original image from 2000 to 3071 and locating the lead beads. These were assigned as "landmark" objects in the object map. The "landmark" and "brain" objects were turned off in the object map and the original image was thresholded from –500 to 2000 to determine "skin." This image was further thresholded using values of 100 to 2000 to extract the bony structure. All object maps were saved to create binary objects for each

of the different tissue types. An example of a completely segmented subject is shown in Figure 11.

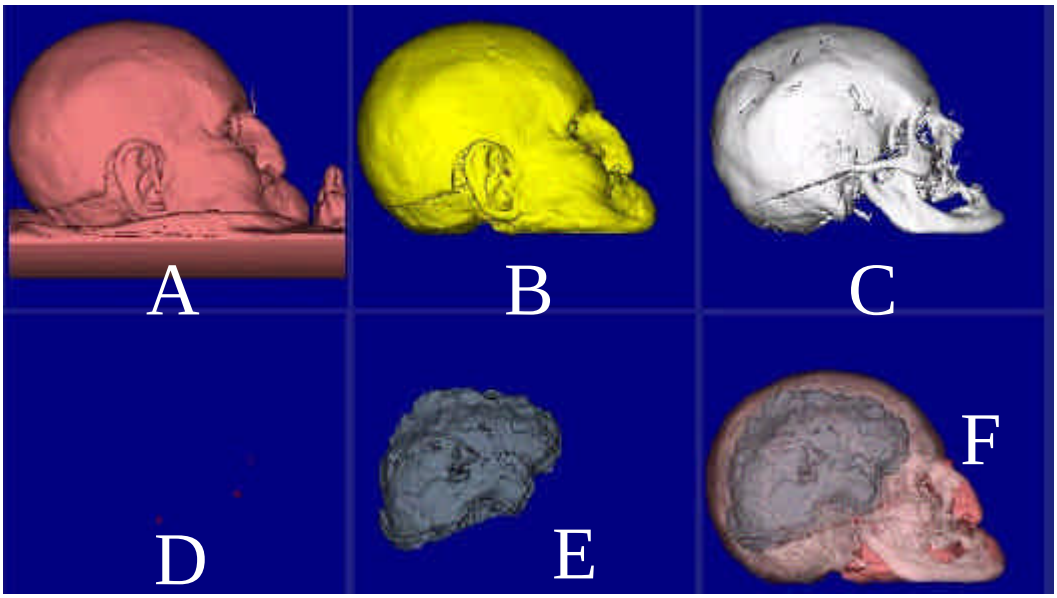

Figure 11: The sequence of segmentation processes used to create separate objects consisting of soft tissue, skull, landmarks, and brain. **A**: the entire CT image including noise, the scanning base, and other bony material placed in front of the face. **B**: the same data with the base, noise, and bony material edited out. **C**: the skull segmented using thresholding. **D**: the landmark data separated from the original CT scan. **E**: the brain has been segmented using thresholding and 3-D morphological operations. **F**: the final segmented head includes object definition for the brain, skull, soft tissue, and landmarks.

The anatomical landmarks were used to initially align the binary objects in the Frankfurt plane with an arbitrary origin as shown in Figure 12.

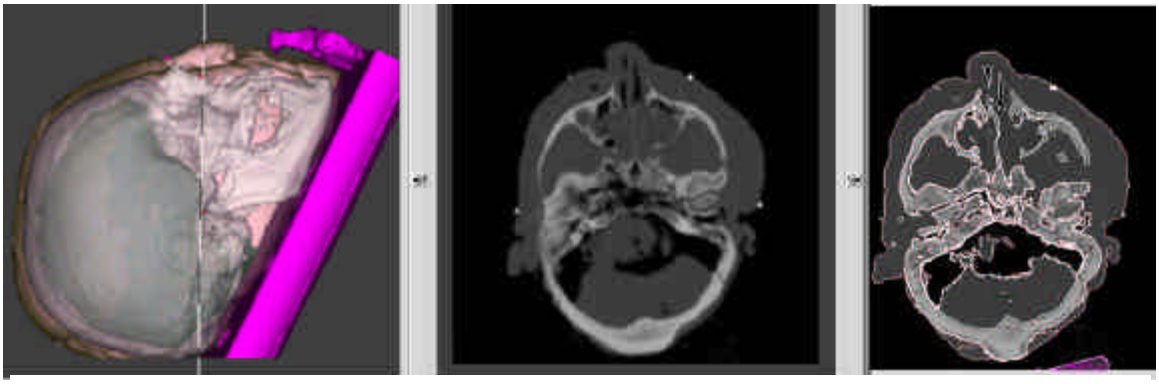

Figure 12: All segmented images were realigned to position them in the Frankfurt plane. Shown in this image is the slice through the plane of the original binary image and the segmented image.

The volume and center of volume measurements were determined for each of the tissue types for each subject. These were saved as .log files and later edited for Excel and Integrate.

Estimation of weight and center of gravity: Mass densities from AMRL-TR-69-70, "Weight, Volume, and Center of Mass of Segments of the Human Body" (Clauser et al., 1969) were used to estimate the weight and center of gravity from these image data. The specific gravity for bone used for the present study was 1.8. Although the cadaver heads were segmented into skull, brain, and soft tissue extraneous to the skull (referred to as "skin"), the soft tissue contains both skin and fat. For this reason, a specific gravity of 0.961 (sg for fat) was used for the "skin" segment. The same specific gravity was used for the brain, as dry brain tissue was not sampled in the Clauser study. The weight and center of gravity measurements were calculated by using the volume data per tissue type output from Analyze with the estimated specific gravity. The weight was calculated by multiplying the volume measurement for each tissue type by the specific gravity. The center of gravity was calculated by editing and importing the landmark files into Integrate, assigning the center of volume measurements for each tissue type, calculating the combined center of gravity using the previously described mass densities, and transforming the results in the Frankfurt plane with the correct origin.

RESULTS

Mass Properties: Direct Measurement

Data tables: Three data tables list the measured mass properties for the female specimens (Table 1), male specimens (Table 2), and a summary for all specimens (Table 3).

A comparison of the mean values for gender of each recorded measure (weight, CG_X, CG_Y, CG_Z) was performed. All comparisons were performed at a significance level of a = 0.05. If the variances of the males and females were found to be not significantly different, then a 2-sample, 2-tailed t-test was performed. Using this statistic, no significant difference was determined for $\mathbf{CG_X}$ {T (13) = 0.59, p = 0.5624}, $\mathbf{CG_Y}$ {T (13) = 0.17, p = 0.8668}, and $\mathbf{CG_Z}$ {T (13) = 0.82, p = 0.4283}.

If the variances of the males and females were found to be significantly different, then an approximate, 2-tailed t-test was performed using Satterthwaite's approximation for degrees of freedom. Using this statistic, a significant difference was determined for the weight {T (7.8) = 3.59, p = 0.0074}.

These statistics indicate that a significant gender difference was found for weight, but not for the centers of gravity.

Table 1**.** Female Specimen Mass Properties

Female Specimens	**Weight** (kg)	$\mathbf{CG_X}$ (cm)	$\mathbf{CG_Y}$ (cm)	$\mathbf{CG_Z}$ (cm)	$\mathbf{MOI_X}$ (kg-cm^2)	$\mathbf{MOI_Y}$ (kg-cm^2)	$\mathbf{MOI_Z}$ (kg-cm^2)
F02	2.98	-0.19	0.48	2.55	83.98	128.16	124.94
F05	2.78	-0.34	0.58	2.86	74.61	112.07	107.97
F06	3	0.42	-0.58	2.18	84.12	123.48	123.48
F07	2.75	-0.5	0.05	3.19	76.52	109.29	111.63
F13	2.78	0.14	-0.04	3.63	102.85	108.70	71.10
F15	3.09	-0.14	-1.1	3.18	87.34	135.18	122.75
F17	2.87	0.76	-0.09	2.81	119.53	120.55	80.76
Mean	2.88	0.02	-0.1	2.91	89.85	119.63	106.09
Std. Dev.	0.13	0.45	0.59	0.47	15.99	10.12	21.74

Table 2. Male Specimen Mass Properties

Male Specimens	**Weight** (kg)	**CG_X** (cm)	**CG_Y** (cm)	**CG_Z** (cm)	**MOI_X** (kg-cm^2)	**MOI_Y** (kg-cm^2)	**MOI_Z** (kg-cm^2)
M09	3.04	-0.11	-0.11	2.29	79.88	129.04	127.58
M10	4.38	0.61	-0.19	2.11	145.43	223.26	233.50
M11	3.53	-0.13	-0.48	2.76	162.40	164.45	110.46
M12	3.96	0.1	-0.22	3.66	124.50	192.97	192.10
M14	3.75	-0.15	0.39	2.25	117.63	174.54	177.03
M18	3.21	0.33	0.34	1.57	142.65	148.64	99.78
M19	2.92	0.17	-0.25	3.8	88.81	129.77	131.38
M20	4.45	0.25	0.05	2.69	151.13	226.48	234.23
Mean	3.68	0.13	-0.06	2.64	126.55	173.64	163.26
Std. Dev.	0.53	0.27	0.3	0.76	29.74	38.27	53.58

Table 3. Overall Specimen Mass Properties

All Specimens	**Weight** (kg)	**CG_X** (cm)	**CG_Y** (cm)	**CG_Z** (cm)	**MOI_X** (kg-cm^2)	**MOI_Y** (kg-cm^2)	**MOI_Z** (kg-cm^2)
Mean	3.27	0.08	-0.08	2.78	109.53	146.64	133.32
Pooled Std. Dev.	0.44	0.36	0.46	0.65	30.18	39.42	50.10

Mass Properties: Measurement from Medical Imaging vs. Direct Measurement

Data tables: One data table lists the summary for all specimens (Table 4). For each measure, the absolute error was determined from the true (directly measured) value to the calculated value (from medical imaging). Since weight and MOI were always positive, absolute percent errors were used. For CG, which has values on both sides of 0, absolute actual errors were used. Subject F13 had an error for CGz that was determined to be an outlier (error = 0.36 cm, next largest error was 0.15 cm) and not used for any analysis (subject had a metal plate in her head – see Figure 13) except for the direction of the error.

The Weibull cumulative distribution was used to model the sample cumulative absolute errors. A description of this distribution is as follows:

Weibull Density Function: $f(x)=\left(\frac{\beta}{\alpha}\right)\left(\frac{x-x_o}{\alpha}\right)^{\beta-1} e^{-\left(\frac{x-x_o}{\alpha}\right)^{\beta}}$ where $0 < \alpha$ and $0 < \beta$

α = scale parameter, β = shape parameter, x_o = lower bound (LB)

Weibull Cumulative Distribution: $F(x)=1-e^{-\left(\frac{x-x_o}{\alpha}\right)^{\beta}}$

Solving the cumulative distribution for X results in the following equation:

$$x = x_o + \alpha * \{-\ln[1-F(x)]\}^{\frac{1}{\beta}}$$

Table 4. Descriptive Statistics And Estimated 50th And 95th Percentiles From The Weibull Distribution.

		Absolute Percent or Actual Error*			Weibull Percentiles		Errors		
							Direction		Sign Test
Measure	N	Min	Mean	Max	50th	95th	Pos	Neg	p-value
Weight	15	0.4	2.8	6.0	2.4	5.8	13	2	0.0074
MOIx	15	1.0	5.1	10.4	4.8	9.0	13	2	0.0074
MOIy	15	2.2	5.5	10.3	5.2	8.9	14	1	0.0010
MOIz	15	0.1	3.1	7.8	2.5	6.2	11	4	0.1185
CGx	15	0.01	0.13	0.29	0.11	0.27	5	10	0.3018
CGy	15	0.01	0.13	0.34	0.09	0.30	9	6	0.6072
CGz	14	0.01	0.07	0.15	0.06	0.16	11	4	0.1185

* For weight and MOI, the errors are percent; for CG, the errors are actual (cm). There was one error for CGz that was removed for being an outlier (error = 0.36 cm), but was used to count the direction of errors. A 2-tailed Fisher's Sign Test was used to determine the significance of a positive or negative bias in the calculated measurements.

Sample Interpretation: For weight, the percent error ranged from 0.4% to 6%. The estimated 50th percentile was 2.4% and the estimated 95th percentile was 5.8%. There was a significant (p = 0.0074) positive bias in the calculated measurement (overestimated the weight). The differences between the measured and calculated values for total head weight estimates ranged from 0.01 kg to 0.18 kg, with an average difference of 0.09 kg (data not shown in Table 4).

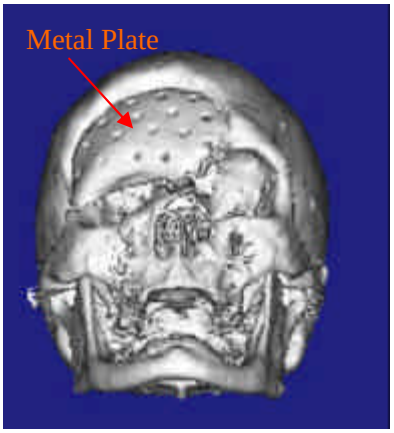

Figure 13: The center of gravity location for this subject was likely skewed by the presence of the metal

In summary, the estimated or calculated values from the medical imaging data when compared to the mechanically measured data resulted in weight percent errors ranging from 0.4% to 6% (mean = 2.8%). Percent errors in MOI ranged from 0.1% to 10.4% (mean = 5.2%). Actual errors in CG ranged from 0.01 cm to 0.34 cm (mean = 0.1 cm). Medical image calculations for weight and MOI had significantly more positive errors than negative errors.

CONCLUSIONS

The method of using medical imaging analysis proved to be a valid, accurate, and

noninvasive means of estimating human head mass properties.

The procedures used to conduct this study consisted of preparing the specimens, marking predetermined landmarks on the head and face, performing anthropometric measures on the specimen, dissecting the head from the neck, measuring the weight and CG with respect to a box coordinate system, digitizing appropriate landmarks on the box and specimens to transform the CG data from the box to the head anatomical coordinate system, performing the CT scans, analyzing the scans, calculating the mass properties of the specimens, and lastly, comparing the two sets of data (directly measured *versus* measured from medical imaging).

The weight, centers of gravity, and principal moments of inertia were directly measured for 15 human cadaveric specimens. All computed tomographic scans were performed and the image data analyzed to estimate the mass properties. Estimations of mass properties were performed using specific gravity values found in current literature.

This study has laid the foundation for using medical imaging to determine mass properties of the human body. Future work will include a similar comparison of the directly measured specimens versus surface scanned (head scanner) data, and magnetic resonance imaging (MRI) data. To increase accuracy, better approximations of tissue densities may be investigated by collecting actual tissue samples of the cadaveric heads, by thresholding within the biomedical imaging software, or by applying more recently published tissue densities. Furthermore, a comparison of these results with past studies will be performed for both mass properties and anthropometry. Finally, estimation of mass properties using medical imaging should be conducted on living human heads to generate a useful set of human head mass properties and anthropometric data.

ACKNOWLEDGMENTS

The authors wish to acknowledge Dr. Randal Ching and Geoff Raynak of the University of Washington, Dr. Del Wilson and Chris Perry of the US Air Force Research Lab - Biodynamics and Acceleration Branch, and Chuck Goodyear of General Dynamics.

This study was completed under the terms of a Cooperative Research and Development Agreement between the US Air Force Research Lab - Biodynamics and Acceleration Branch, Wright-Patterson AFB, OH, and the University of Washington's Orthopaedic & Biomechanics Lab.

REFERENCES

BAUGHN, D. J., ALBERY, C. B., and KALEPS, I. (1995). The standard automated mass properties (STAMP) measurement testing and calibration procedures, AL/CF-TR-1995-0091, Armstrong Laboratory, Wright-Patterson AFB, Ohio.

BECKER, E. D. (1972). Measurement of mass distribution parameters of anatomical segments. Proc. 16th Stapp Car Crash Conference, SAE Paper No. 720964, 81(4), pp. 2818-2833.

BEIER, G., SCHULLER, E., SCHUCK, M., EWING, C. L., BECKER, E. D., and THOMAS, D. J. (1980). Center of gravity and moments of inertia of human heads. Proc. 5th Int. IRCOBI Conference on the Biomechanics of Impact, p. 228.

CHANDLER, R. F., CLAUSER, C. E., MCCONVILLE, J. T., REYNOLDS, H. M., and YOUNG, J. W. (1974). Investigation of inertial properties of the human body. AMRL-TR-74-137. Aerospace Medical Research Laboratory, Wright-Patterson AFB, Ohio.

CLAUSER, C. E., MCCONVILLE, J. T., and YOUNG, J. W. (1969). Weight, volume, and center of mass of segments of the human body. AMRL-TR-69-70. Aerospace Medical Research Laboratory, Wright-Patterson AFB, Ohio.

HARLESS, E., (1860). The static moments of the component masses of the human body. Trans. of the Math-Phys., Royal Bavarian Acad. of Sci., 8(1), pp. 69-96. Unpublished English Translation, FTD-TT-61-295, Wright-Patterson AFB, Ohio.

KALEPS, I., CLAUSER, C. E., YOUNG, J. W., CHANDLER, R. F., ZEHNER, G. F., and MCCONVILLE, J. T. (1984). Investigation into the mass distribution properties of the human body and its segments. Ergonomics, 27(12), pp. 1225-1237.

KNOX III, F. S., BUHRMAN, J. R., and PERRY, C. E. (1992). Biomechanics of ejection safety for night vision systems. Proc. Night Vision 92, London, U.K.

MCCONVILLE, J. T., CHURCHILL, T. D., KALEPS, I., CLAUSER, C. E., and CUZZI, J. (1980). Anthropometric relationships of body and body segment moment of inertia. AFAMRL-TR-80-119. Air Force Aerospace Medical Research Laboratory, Wright-Patterson AFB, Ohio.

SCHULTZ, R. B., OBERGEFELL, L. A., RIZER, A. L., ALBERY, C. B., and ANDERSON, B. A., (1997). Comparison of measured and predicted human whole-body inertial properties. Proc. 41st Stapp Car Crash Conference, SAE Paper No. 97S-57.

SELF, B. P., SPITTLE, E. K., KALEPS, I., and ALBERY, C.B. (1992). Accuracy and repeatability of the standard automated mass properties measurement system. AL-TR-1992-0137. Armstrong Laboratory, Wright-Patterson AFB, Ohio.

WALKER, L. B., HARRIS, E. H., and PONTIUS, U. R., (1973). Mass, volume, center of mass and mass moment of inertia of head and head and neck of human body. Final Report, AD 762 581. Dept. of Navy, Office of Naval Research, Washington, D.C.

WHITESTONE, J. J. and ALBERY, C. B. (1996). Assessment of the hybrid II manikin headform as a reference for mass properties measurements of helmet systems. SAFE J., 26(3), pp. 9-17.

DISCUSSION

PAPER: **Comparison of Cadaveric Human Head Mass Properties: Mechanical Measurement vs. Calculation from Medical Imaging**

PRESENTER: ***Christopher Albery, General Dynamics***

QUESTION: *Guy Nusholtz, Daimler/Chrysler*
What do you mean by "naturally drained?"

ANSWER: Just due to gravity. All the fluids were drained out at IIAM

Q: But, you have air spaces, then.

A: Absolutely.

Q: Inside of the skull. So, your density is including them, that air?

A: Yes. Well, for each tissue type. So really, any of these voids were accounted for, but that was a major consideration the condition of the specimen, especially the brain. The brain had really wasted and left quite a void.

Q: So you've got--You've got some large voids in the brain which you were somehow able to account for, but the micro voids that accumulate inside of the tissue, either through decay or whatever process, is not accounted for?

A: No. If there was tissue, it was accounted for. The absence of tissue did not factor into the estimates. The densities were actually just assigned from what was available in Clauser publication. So looking back on this, that's something that next time we go through it, we're either going to have to sample from the specimens or use better published. More than likely, though, what we'll do is we'll take--analyze and go in there and zero in on the specific tissue types and densities.

Q: So, you'll try and get an actual measurement, a measurement of the density and then use that--

A: Right. But I mean if we actually did this on living humans, we'd most likely be able to use published data.

Q: For the density?

A: For the densities. Or again, we could use analyze and we'd go through and actually do the calculation.

Q: Then, how did your--You're relatively close and yet you've got a density which shouldn't match. How do you account for? In other words--

A: Just the nature of the head being spherical, I think that helps. And for CG, you notice it was pretty much right on. But then you start taking into account the moments, and you have that distance and that weight, so it's very important at that point.

Q: That makes sense. Thank you.